Recognition of DNA Base Pair Mismatches by a Cyclometalated Rh(III) Intercalator

ARTICLE *in* INORGANIC CHEMISTRY · NOVEMBER 2000

Impact Factor: 4.76 · DOI: 10.1021/ic000549z · Source: PubMed

2 AUTHORS:

Jennifer Kisko

9 PUBLICATIONS **282** CITATIONS

SEE PROFILE

Jacqueline K Barton

California Institute of Technology

391 PUBLICATIONS **31,473** CITATIONS

SEE PROFILE

Recognition of DNA Base Pair Mismatches by a Cyclometalated Rh(III) Intercalator

Jennifer L. Kisko and Jacqueline K. Barton*

Division of Chemistry and Chemical Engineering, California Institute of Technology, Pasadena, California 91125

Received May 23, 2000

Two cyclometalated complexes of Rh(III), *rac*-$[Rh(ppy)_2chrysi]^+$ and *rac*-$[Rh(ppy)_2phi]^+$, have been synthesized and characterized with respect to their binding to DNA. The structure of *rac*-$[Rh(ppy)_2phi]Cl\cdot H_2O\cdot CH_2Cl_2$ has been determined by X-ray diffraction (monoclinic, $P2_1/c$, $Z = 4$, $a = 18.447(3)$ Å, $b = 9.770(1)$ Å, $c = 17.661(3)$ Å, $\beta = 94.821(11)°$, $V = 3172.0(8)$ Å^3) and reveals that the complex is a distorted octahedron with nearly planar ligands, similar in structure to the DNA mismatch recognition agent $[Rh(bpy)_2chrysi]^{3+}$. The 2-phenylpyridyl nitrogen atoms are shown to be in the axial positions, as a result of trans-directing effects. This tendency simplifies the synthesis and purification of such complexes by limiting the number of possible isomers generated. The abilities of $[Rh(ppy)_2chrysi]^+$ and $[Rh(ppy)_2phi]^+$ to bind and, with photoactivation, to cleave DNA have been demonstrated in assays on duplex DNA in the absence and presence of a single CC mismatch. $[Rh(ppy)_2chrysi]^+$ was shown upon photoactivation to cleave DNA selectively at the base pair mismatch whereas $[Rh(ppy)_2phi]^+$ cleaves B-DNA nonspecifically. The reactivity of $[Rh(ppy)_2chrysi]^+$ was also compared to that of the known mismatch recognition agent $[Rh(bpy)_2chrysi]^{3+}$. Competitive photocleavage studies revealed that a 14-fold excess of $[Rh(ppy)_2chrysi]^+$ was required to achieve the same level of binding as that of $[Rh(bpy)_2chrysi]^{3+}$. However, the ratio of damage induced by $[Rh(bpy)_2chrysi]^{3+}$ to that induced by $[Rh(ppy)_2chrysi]^+$ is considerably greater than this value, indicating that decreased photoefficiency for the cyclometalated complex must contribute to its significantly attenuated photoreactivity. These cyclometalated intercalators provide the starting points for the design of a new family of metal complexes targeted to DNA.

Introduction

Cyclometalated octahedral ruthenium ($4d^6$), rhodium ($4d^6$), and iridium ($5d^6$) complexes have been widely studied with particular emphasis placed on their photoelectrochemical, photophysical, redox, and spectroscopic properties.[1] The changes in such properties observed upon the replacement of a typical N,N-donor ligand such as 2,2′-bipyridine with its carbocylic structural analogue, 2-phenylpyridine (ppy), have been of particular interest.[2] Replacing 2,2′-bipyridine with 2-phenylpyridine, a C,N-donor due to its σ-donor/π-acceptor properties, results in higher energy d−d excited states and increasingly lower energy metal-to-ligand charge transfer states as well as a decrease in overall charge with increasing number of M−C σ-bonds.[1,3]

This laboratory has focused on the design of metallointercalators containing functionalized polypyridyl ligands to achieve site-specific DNA recognition.[4] A general problem in this effort has been the synthesis of reasonable quantities of the metal complex isomer of interest, given the abundance of isomers created when using nonsymmetric bidentate ligands. One advantage of using (C∧N) cyclometalating ligands is their tendency to bind with the nitrogen in the axial position, greatly reducing the number of possible isomers. This preferred mode of coordination may thus provide a simplified route to the functionalization of DNA intercalators. Although the photochemistry of cyclometalated complexes has been studied for many years, few studies of the photochemical reactivity of such complexes have been reported, and no studies of the reactivity of cyclometalated Rh(III) complexes with DNA have been reported.[5]

Metallointercalators of the type $[RhL_2(phi)]^{3+}$ have been shown to be effective in binding DNA by inserting[6] the 9,10-phenanthrene quinone diimine (phi) moiety between base pairs in the DNA duplex.[4] A recent crystal structure of a phi complex of rhodium bound to a DNA octamer shows the phi ligand deeply inserted and stacked within the duplex from the major

* To whom correspondence should be addressed.

(1) Steel, P. J. *J. Organomet. Chem.* **1991**, *408*, 395−402. (b) Sprouse, S.; King, K. A.; Spellane, P. J.; Watts, R. J. *J. Am. Chem. Soc.* **1984**, *106*, 6647−6653. (c) Ohsawa, Y.; Sprouse, S.; King, K. A.; DeArmond, M. K.; Hanck, K. W.; Watts, R. J. *J. Phys. Chem.* **1987**, *91*, 1047−1054. (d) Garces, F. O.; King, K. A.; Watts, R. J. *Inorg. Chem.* **1988**, *27*, 3464. (e) Arz, C.; Pregosin, P. S.; Anklin, C. *Magn. Reson. Chem.* **1987**, *25*, 158. (f) Zilian, A.; Maeder, U.; von Zelewsky, A.; Gudel, H. U. *J. Am. Chem. Soc.* **1989**, *111*, 3855. (g) Sandrini, D.; Maestri, M.; Ciano, M.; Maeder, U.; von Zelewsky, A. *Helv. Chim. Acta* **1990**, *73*, 1306.

(2) Reveco, P. H.; Medley, J. H.; Garber, A. R.; Bhacca, N. S.; Selbin, J. *Inorg. Chem.* **1985**, *24*, 1096. (c) Constable, E. C.; Holmes, J. M. *J. Organomet. Chem.* **1986**, *301*, 203.

(3) Colombo, M. G.; Brunold, T. C.; Riedener, T.; Gudel, H. U. *Inorg. Chem.* **1994**, *33*, 545−550. (b) Colombo, M. G.; Gudel, H. U. *Inorg. Chem.* **1993**, *32*, 3081−3087.

(4) Erkkila, K. E.; Odom, D. T.; Barton, J. K. *Chem. Rev.* **1999**, *99*, 2777−2796. (b) Johann, T.; Barton, J. K. *Philos. Trans. R. Soc. London, Ser. A* **1996**, *354*, 299.

(5) The cytotoxicity of a (C∧N) cyclometalated Pt(II) complex, [Pt(dppz)(tN∧C)][CF_3SO_3], in carcinoma cell lines was recently reported: Che, M.-C.; Yang, M.; Wong, K.-H.; Chan, H.-L.; Lam, W. *Chem.—Eur. J.* **1999**, *5*, 3350. (b) The interaction of cyclometalated Pt(II) and Pd(II) complexes with DNA and their respective cytotoxicities have been studied: (i) Quiroga, A. G.; Perez, J. M.; Lopez-Solera, I.; Masaguer, J. R.; Luque, A.; Román, P.; Edwards, A.; Alonso, C.; Navarro-Ranninger, C. *J. Med. Chem.* **1998**, *41*, 1399−1408. (ii) Navarro-Ranninger, C.; Lopez-Solera, I.; Gonzales, V. M.; Pérez, J. M.; Alvarez-Valdés, A.; Martín, A.; Raithby, P. R.; Masaguer, J. R.; Alonso, C. *Inorg. Chem.* **1996**, *35*, 5181−5187.

(6) Lerman, L. S. *J. Mol. Biol.* **1961**, *3*, 18−30.

10.1021/ic000549z CCC: $19.00
Published on Web 09/21/2000

groove side.[7] Such complexes of rhodium are known to promote direct DNA strand scission via hydrogen abstraction from deoxyribose.[8] The chemistry of such intercalators has been extensively investigated through the variation in ancillary ligands (L), such as ethylenediamine, phenanthroline, and 4,4′-diphenyl-2,2′-bipyridyl, that allow sequence-specific targeting of DNA.[9] Although it is intercalation of the phi ligand in the major groove of DNA that provides binding affinity, it is shape selectivity (indirect readout) and/or interaction with base functionalities and appropriately positioned substituents on the ancillary ligands (direct readout) that can generate sequence selectivity. One example of such shape selectivity is the preferential binding of the Δ-isomer of octahedral intercalators to right-handed B-DNA; such intercalation of the corresponding Λ-isomer is more hindered due to unfavorable steric interactions with the phosphate backbone.[10] Several studies have also been conducted in which the ancillary ligands are functionalized to lend greater specificity by increasing the number of interactions in the major groove. For example, the complex Δ-α-[Rh(*R*,*R*)-Me_2trien](phi)$^{3+}$ (Me_2trien = (2*R*,9*R*)-diamino-4,7-diazadecane) has been used in direct readout studies to target the sequence 5′-TGCA-3′; here functionalization of the ancillary ligands with methyl groups leads to specific van der Waals interactions.[11] High-resolution NMR studies[12] and more recently the crystal structure[7] of the metallointercalator bound to its target site have confirmed these sequence-directing interactions.

Another example of shape-selective recognition is seen in the site-specific binding by the DNA intercalator bis(2,2′-bipyridyl)(5,6-chrysenequinone diimine)rhodium(III), [Rh(bpy)$_2$chrysi]$^{3+}$. This complex selectively targets base pair mismatches and, upon photoactivation, cleaves the DNA backbone at the target site.[13] Remarkably, the complex was found to be specific for a single mismatched site in a linearized plasmid containing 2725 base pairs. Base pair mismatches can occur in DNA as a result of either errors in replication or externally induced mutation. Such errors are typically corrected by mismatch repair proteins (MMR).[14] A signature of certain cancers such as hereditary nonpolyposis colorectal and some breast cancers is that such repair systems are severely compromised. The presence of mismatches in the DNA sequence due to MMR deficiency may afford a unique opportunity for cell targeting by small molecules.

[Rh(bpy)$_2$chrysi]$^{3+}$ was found to induce strand scission at approximately 80% of all mismatch types in all possible surrounding sequence contexts.[13] This specificity is largely due to shape selection; the four-ring intercalating ligand (chrysi) is too bulky to intercalate in normal B-DNA base steps but can do so near mismatched DNA base pairs which are destabilized as a result of the disruption of the regular B-DNA structure. This broad activity is promising for the design of a mismatch-specific intercalator, but the overall charge on [Rh(bpy)$_2$chrysi]$^{3+}$ is quite high for therapeutic application.[15] Thus, our efforts have been directed toward the synthesis of a similar intercalator capable of highly selective mismatch recognition, yet lower in overall charge effected by the incorporation of cyclometalating C,N-donor ligands.

Detailed here is the first study of the photochemistry of cyclometalated Rh(III) complexes with DNA. Concomitantly, we describe the synthesis and study of a new agent of base pair mismatch recognition with greater therapeutic potential.

Experimental Section

Materials. Commercially obtained chemicals were used as received. 2-Phenylpyridine, 9,10-diaminophenanthrene, and $SnCl_2 \cdot 2H_2O$ were purchased from Aldrich. $RhCl_3 \cdot 2H_2O$ was obtained from Pressure Chemical. Chrysene was purchased from Acros Chemicals. 5,6-Chrysenequinone was prepared according to literature procedure.[16]

Instrumentation. Electronic spectra were recorded on a Beckman DU 7400 UV−visible spectrophotometer. Mass spectra (electrospray ionization) were measured on an LCQ mass spectrometer. High-performance liquid chromatography (HPLC) was performed on a Waters 996 system using a Vydac C_{18} column (4.0 mL/min liquid phase, linear gradient over 50 min from 100% 50 mM NH_4OAc, pH 7.0 to 100% acetonitrile). NMR spectra were recorded on a Varian 500 MHz instrument. DNA synthesis was performed on an ABI 392 DNA/RNA synthesizer using reagents from Glen Research. DNA was purified using Glen Research Poly-Pak II cartridges following the manufacturer's protocol. Photocleavage reactions were carried out using a 1000 W Oriel Hg/Xe arc lamp with a monochromator fitted with a 300 nm cutoff filter and an IR filter.

Synthesis and Characterization. (a) *rac*-[Rh(ppy)$_2$phi]Cl (Bis(2-phenylpyridine)9,10-phenanthrenequinone Diimine Rhodium(III) Chloride). Bis(bis(2-phenylpyridine) rhodium(III) chloride), [Rh(ppy)$_2$Cl]$_2$ (500 mg, 0.560 mmol), prepared according to literature procedure,[1b] was dissolved after 30 min of stirring in 40 mL of dichloromethane (DCM) at ambient temperature. 9,10-Diaminophenanthrene (310 mg, 1.49 mmol) in 35 mL of acetonitrile was added to the yellow solution, producing a blue-green color that quickly changed to yellow-brown. The reaction was allowed to stir at ambient temperature for 12 h. After the solvents were removed in vacuo, the yellow-brown powder was extracted into water and filtered. The filtrate was loaded on a CM-C25 Sephadex cation exchange column (resin equilibrated with 0.05 M $MgCl_2$). After the brown band was rinsed with copious amounts of water and salt concentrations were ramped up to 0.3 M $MgCl_2$, the product was eluted from the resin with dimethylformamide (DMF). The solvent was removed in vacuo to yield the product as a brown solid. The solid was extracted into a 1:1 dichloromethane/ethyl acetate solution, filtered, and allowed to stand at ambient temperature until dark red crystals of the product were deposited (220 mg, 30%). ^{1}H NMR (d_6-DMSO, 500 MHz): δ 13.0 (s), 8.65 (m), 8.45 (m), 8.25 (m), 8.15 (m), 8.05 (m), 7.90 (m), 7.75 (m), 7.55 (m), 7.30 (m), 7.0 (m), 6.85 (m), 6.10 (m). MS (electrospray): 617.1 ($M^+ - Cl$), 411.1 ($M^+ - Cl -$ (phi)). UV−vis (H_2O, pH 5) (nm, (M^{-1} cm^{-1})): 245, (59 300); 263 (sh), (52 400); 368, (12 700); 413, (13 000).

(b) *rac*-[Rh(ppy)$_2$chrysi]Cl (Bis(2-phenylpyridine)5,6-chrysenequinone Diimine Rhodium(III) Chloride). 5,6-Diaminochrysene hydrochloride (DAC HCl) was first prepared analogously to 9,10-diaminophenanthrene hydrochloride (DAP HCl).[17a] It appears, however,

(7) Kielkopf, C. L.; Erkkila, K. E.; Hudson, B. P.; Barton, J. K.; Rees, D. C. *Nat. Struct. Biol*. **2000**, *7*, 117−121.
(8) Sitlani, A.; Long, E. C.; Pyle, A. M.; Barton, J. K. *J. Am. Chem. Soc.* **1992**, *114*, 2303−2312.
(9) Sitlani, A.; Dupureur, C. M.; Barton, J. K.; *J. Am. Chem. Soc.* **1993**, *115*, 12589−12590. (b) Sitlani, A.; Barton, J. K. *Biochemistry* **1994**, *33*, 12100−12108. (c) Shields, T. P.; Barton, J. K. *Biochemistry* **1995**, *34*, 15037−15048.
(10) Barton, J. K. *Science* **1986**, *233*, 727−734.
(11) Krotz, A. H.; Hudson, B. P.; Barton, J. K. *J. Am. Chem. Soc.* **1993**, *115*, 12577−12578.
(12) Hudson, B. P.; Barton, J. K. *J. Am. Chem. Soc.* **1998**, *120*, 6877−6888. (b) Hudson, B. P.; Dupureur, C. M.; Barton, J. K. *J. Am. Chem. Soc.* **1995**, *117*, 9379−9380.
(13) Jackson, B. A.; Barton, J. K. *J. Am. Chem. Soc.* **1997**, *119*, 12986−12987. (b) Jackson, B. A.; Alekseyev, V. Y.; Barton, J. K. *Biochemistry* **1999**, *38*, 4655−4662.
(14) Kolodner, R. *Genes Dev.* **1996**, *10*, 1433−1442. (b) Modrich, P. *Annu. Rev. Genet.* **1991**, *25*, 229−253. (c) Modrich, P. *Science* **1994**, *266*, 1959−1960. (d) Kolodner, R. D. *Trends Biochem. Sci.* **1995**, *20*, 397−401.
(15) Dwyer, F. P.; Wright, R. D.; Gyarfas, E. C.; Shulman, A. *Nature* **1957**, *179*, 425−426. (b) Farnsworth, P. G.; Shulman, A.; Casey, A. T. *Chem.-Biol. Interact.* **1977**, *18*, 289−294. (c) Capnick, L. B.; Chasin, L. A.; Raphael, R. L.; Barton, J. K. *Mutat. Res.* **1988**, *201*, 17−26.
(16) Greabe, V. C.; Honigsberger, F. *Justus Liebigs Ann. Chem.* **1900**, *311*, 257−265.
(17) Schmidt, J.; Soell. *Chem. Ber*. **1908**, *41*, 3684. (b) Junicke, H.; Barton, J. K. Unpublished results.

that as a result of steric crowding only a low yield of the diimine is obtained, the monoamine being favored.[17b] A round-bottom flask under argon was charged with the crude product (100 mg) immediately after preparation, and $[Rh(ppy)_2Cl]_2$ (100 mg, 0.112 mmol) was added. Degassed acetonitrile (10 mL) was then introduced, and the yellow suspension was allowed to stir at ambient temperature for 30 min. Degassed saturated aqueous sodium carbonate (5 mL) was then added. The suspension slowly turned red-brown and was allowed to stir under argon at ambient temperature followed by 5 days at 50 °C before opening to air and allowing the mixture to stir at room temperature for 3 days. The product (4 mg, 10%) was purified by HPLC (0−50 min, 100% 100 mM NH_4OAc to 100% acetonitrile). ^1H NMR (d_6-DMSO, 500 MHz): δ 13.0 (s), 12.6 (s), 8.6 (d), 8.5 (t), 8.4 (m), 8.3 (t), 8.15 (d), 8.10 (t), 8.05 (m), 8.0 (m), 7.80 (t), 7.55 (m), 7.4 (t), 7.3 (t), 7.2 (t), 7.0 (m), 6.9 (m), 6.25 (d), 6.10 (d). MS (electrospray): 667.0 ($M^+ - Cl$), 411.1 ($M^+ - Cl -$ (chrysi)). UV−vis (acetonitrile/water) (nm): 247.9, 262.0, 370.1, 423.0. The extinction coefficients determined for $[Rh(ppy)_2phi]^+$ were taken to be the same as those for $[Rh(ppy)_2chrysi]^+$ in the ultraviolet and were used to determine the concentration of solutions of $[Rh(ppy)_2chrysi]^+$.

Single-Crystal X-ray Diffraction Characterization of *rac*-[Rh(ppy)$_2$phi]Cl·H$_2$O·CH$_2$Cl$_2$. [Rh(ppy)$_2$phi]Cl was extracted into a 1:1 DCM/EtOAc solution from which dark red concave block crystals were deposited. A concave corner of a crystal was cut and mounted on a Bruker SMART 1000 ccd diffractometer (SAINT v6.02). Absorption and decay corrections were not used. No reflections were omitted from the final data set. The $\sigma^2(F_o^2)$ values include the default instrument error constant of 0.005*I*. The structure was solved using direct methods with SHELXS-97.[18] The protons of the dichloromethane solvent molecule were placed on calculated positions and were constrained to ride on the atom to which they are attached ($1.2u_{eq}$). No protons were calculated for the disordered water molecule. The positions of all the other hydrogen atoms were taken from difference Fourier maps and refined with 1.2 times the u_{eq} value of the attached atom. All non-hydrogen atoms were refined with anisotropic thermal parameters. A series of full-matrix least-squares refinement cycles on F^2 (program SHELXL-97) followed by Fourier syntheses gave all remaining atoms.[18] Further details are listed in Table 1.

The asymmetric unit contains one water and one dichloromethane molecule as well as one $[Rh(ppy)_2phi]Cl$ unit. The Cl^- ions and water molecules are disordered. One population parameter was used for all four sites: either $x(Cl^-\cdot H_2O)$ in two sites or $(1 - x)(H_2O\cdot Cl^-)$ in two sites shifted by ∼0.7−0.8 Å from the first pair.

The determination of the carbon and nitrogen ligating atoms was made by refinement of relative populations. Upon completion of refinement, the identities of the carbons and nitrogens were switched and refinement was repeated. Each carbon or nitrogen was restrained to have the same coordinates and displacement parameters. The refinements resulted in the following site populations: N3 (1.05N, −0.05C); N4 (1.01N, −0.01C); C25 (−0.05N, 1.05C); C36 (−0.05N, 1.05C).

DNA Preparation and Photocleavage Experiments. The 29-mer DNA hairpins, 21-mer, and 31/41-mer duplexes were synthesized on an ABI 392 DNA/RNA synthesizer, using standard phosphoramidite synthesis,[19] and were initially purified on Poly-Pak II cartridges and further purified by HPLC (98% 100 mM NH_4OAc/2% acetonitrile to 70% 100 mM NH_4OAc/30% acetonitrile over 30 min). The hairpins and single strands were then 5′-labeled with [^{32}P]ATP and polynucleotide kinase. The labeled strands were further purified by gel electrophoresis (20% denaturing polyacrylamide gel), eluted from the gel via soaking in TE, ethanol precipitated, and annealed in the presence of unlabeled DNA. The labeled DNA 21-mer duplex (20 μM in 10 mM Tris pH 8.0, 4 mM NaOAc, 3.6 mM NaCl) was treated with either $[Rh(ppy)_2phi]Cl$ or $[Rh(bpy)_2phi]Cl_3$ in 10 mM Tris, pH 8.0, and irradiated at 313 nm. The labeled hairpins were treated with either $[Rh(ppy)_2chrysi]Cl$ or $[Rh(bpy)_2phi]Cl_3$ in 10 mM Tris, pH 8.0, and were irradiated at 313 nm. The labeled 31/41-mer duplex (20 μM in 10 mM Tris pH 8.0, 4 mM NaOAc, 3.6 mM NaCl) was treated with either $[Rh(ppy)_2chrysi]Cl$ or $[Rh(bpy)_2phi]Cl_3$ in 10 mM Tris, pH 8.0, and irradiated. After irradiation, all samples were lyophilized, denaturing formamide loading dye was added, and the samples were electrophoresed on a 20% polyacrylamide denaturing gel. The photocleavage results were observed via phosphorimagery (Molecular Dynamics Phosphorimager).

Table 1. Crystal Data and Structure Refinement for $[Rh(ppy)_2Phi]^+Cl^-\cdot H_2O\cdot CH_2Cl_2$

empirical formula	$C_{37}H_{30}Cl_3N_4ORh$
formula weight	755.94
crystal habit	concave block
crystal size	$0.33 \times 0.24 \times 0.20$ mm^3
crystal color	deep ruby red
type of diffractometer	Bruker SMART 1000 ccd
wavelength	0.71073 Å Mo Kα
data collection temperature	98 K
unit cell dimensions	a =18.447(3) Å b = 9.7707(12) Å c = 17.661(3) Å $\alpha = 90°$ $\beta = 94.821(11)°$ $\gamma = 90°$
volume	3172.0(8) Å^3
Z	4
crystal system	monoclinic
space group	$P2_1/c$
density (calculated)	1.583 g/cm^3
θ range for data collection	2.22−28.79° ($\pm h$, $\pm k$, ± 1)
data collection scan type	ω-scans at 4 fixed ϕ values
reflections collected	38038
independent reflections	7690 [$R_{int} = 0.0453$]
observed reflections [$I > 2\sigma(I)$]	6462
parameters	512
absorption coefficient	0.830 mm^{-1}
absorption correction	none
refinement method	full-matrix least-squares on F^2
goodness-of-fit on F^2	2.841
final R indices [$I > 2\sigma(I)$]	R1 = 0.0375, wR2 = 0.0777
R indices (all data)	R1 = 0.0474, wR2 = 0.0790
largest diff peak and hole	1.310 and −0.964 e Å^{-3}

Results

Synthesis and Spectral Characterization. Two new cyclometalated Rh(III) complexes, $[Rh(ppy)_2phi]Cl$ and $[Rh(ppy)_2chrysi]Cl$, have been prepared (Figure 1). $[Rh(ppy)_2phi]Cl$ was synthesized via the addition of commercially available 9,10-diaminophenanthrene to the dichlorodimer, $[Rh(ppy)_2Cl]_2$, in DMF in the presence of atmospheric oxygen. The product was purified by crystallization from a concentrated 1:1 dichloromethane/ethyl acetate solution with an overall yield of 30%.

The synthesis of $[Rh(ppy)_2chrysi]Cl$ involved the *in situ* generation of the air-sensitive 5,6-diaminochrysene. The hydrochloride salt of 5,6-diaminochrysene, prepared analogously to that of 9,10-diaminophenanthrene, was added to the dichlorodimer in acetonitrile and subsequently treated with sodium carbonate. The reaction mixture was allowed to stir under an inert atmosphere at 50 °C, and after oxidation in the presence of atmospheric oxygen the product was isolated by HPLC.

The UV−visible spectra of $[Rh(bpy)_2phi]Cl_3$ and $[Rh(ppy)_2phi]Cl$ at pH 4 are shown in Figure 2a. At pH 4, the ligand-to-metal charge transfer (LMCT) band of $[Rh(bpy)_2phi]Cl_3$ has an absorbance maximum at 379 nm. However, the spectrum of $[Rh(ppy)_2phi]Cl$ shows two such absorbances at pH 4, one at 368 and another at 413 nm. In addition, two relatively intense peaks are observed at 304 and 316 nm only for the bpy analogue;

(18) Sheldrick, G. M. *SHELX-97, Programs for Crystal Structure Determination and Refinement*; University of Göttingen, Göttingen, Germany, 1997.

(19) Caruthers, M. H.; Barone, A. D.; Beaucage, S. L.; Dodds, D. R.; Fisher, E. F.; McBride, L. J.; Matteucci, M.; Stabinsky, Z.; Tang, J.-Y. *Methods Enzymol.* **1987**, *154*, 287.

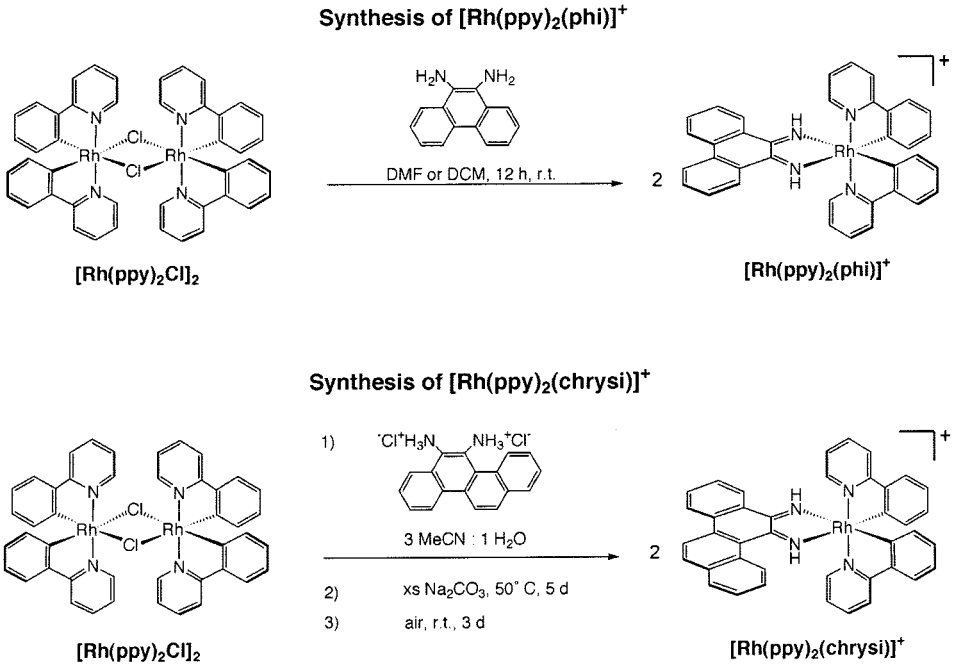

Figure 1. Syntheses of [Rh(ppy)$_2$phi]Cl (top) and [Rh(ppy)$_2$chrysi]Cl (bottom).

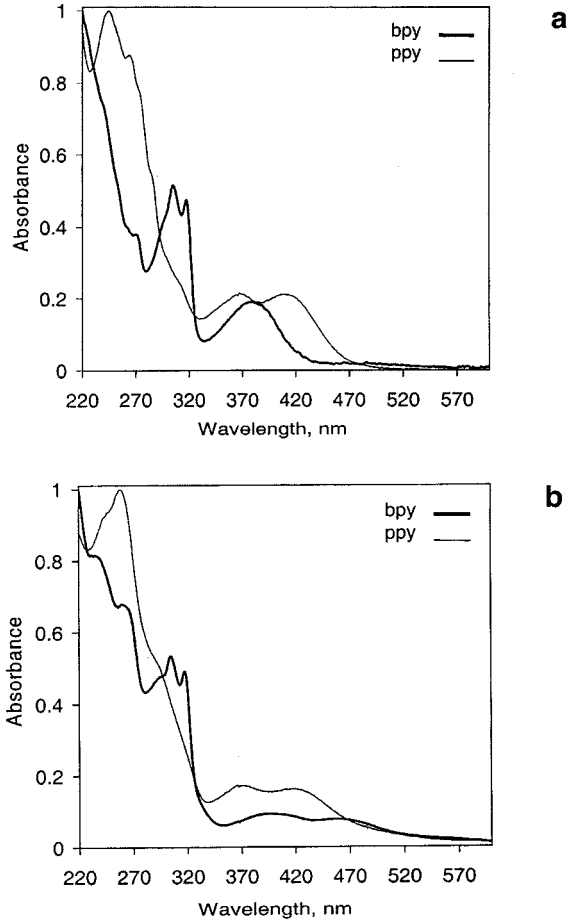

Figure 2. UV−visible spectra of (a) [Rh(bpy)$_2$phi]Cl$_3$ vs [Rh(ppy)$_2$phi]Cl and (b) [Rh(bpy)$_2$chrysi]Cl$_3$ vs [Rh(ppy)$_2$chrysi]Cl. Spectra were obtained in aqueous HCl at pH 4.

as there are no equivalent absorbances in the cyclometalated complexes, they are presumably due to the bipyridyl ligands.

The UV−visible spectra of both [Rh(bpy)$_2$chrysi]Cl$_3$ and [Rh(ppy)$_2$chrysi]Cl at pH 4 are shown in Figure 2b. The spectrum of [Rh(bpy)$_2$chrysi]Cl$_3$, which has a pK_a of 5.2, shows two LMCT transitions at 399 and 462 nm under acidic conditions. At basic pH, its spectrum shows only one blue-shifted LMCT transition at 384 nm. The corresponding phi complex, [Rh(bpy)$_2$phi]Cl$_3$ (shown in Figure 2a), shows only one such transition under acidic as well as basic conditions but also shows a blue-shifting of the LMCT absorption band upon elevation of pH. This difference has been attributed to the inequivalence of the imino protons of the chrysi complex which are present only under acidic conditions.[20] The spectrum of [Rh(ppy)$_2$chrysi]Cl in Figure 2b shows two LMCT bands at 370 and 423 nm, both slightly red-shifted compared to those of the corresponding phi complex at 368 and 413 nm. However, increasing the pH had no significant effect on the spectra of the cyclometalated complexes up to pH 12, indicating that deprotonation does not occur within this range. Because the electron density at the metal center is much higher for the cyclometalated complexes as a result of the M−C σ-bonds, these complexes are much less likely to be deprotonated under basic conditions. Nonetheless, both the cyclometalated phi and chrysi complexes show two LMCT absorbances whereas for the bipyridyl phi and chrysi complexes, only the chrysi complex under acidic conditions shows two such transitions. Perhaps the reduction in complex symmetry, which occurs with both chrysi deprotonation and ppy coordination, accounts for the increase in the number of transitions.

On the basis of UV−visible and NMR spectra, both [Rh(ppy)$_2$phi]Cl and [Rh(ppy)$_2$chrysi]Cl are stable in aqueous solution in air. Titrations as a function of pH reveal that the complexes are unaffected by high pH conditions (pH 12) but decompose at low pH; presumably, under acidic conditions the ppy ligand can be reprotonated and dissociates.

Crystallographic Characterization of [Rh(ppy)$_2$phi]Cl. An ORTEP diagram of [Rh(ppy)$_2$phi]$^+$ is shown in Figure 3 based upon the X-ray diffraction analysis of the crystal structure. Details of the structure determination are given in Table 1.

A critical issue with respect to the structure of the cyclo-

(20) Jackson, B. A.; Henling, L. M.; Barton, J. K. *Inorg. Chem.* **1999**, *38*, 6218−6224.

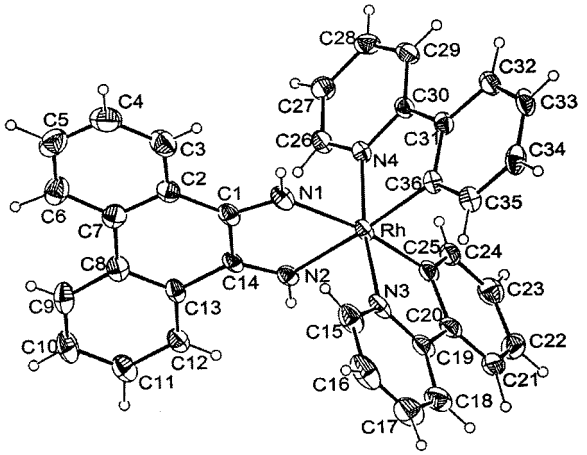

Figure 3. Labeled ORTEP drawing of $[Rh(ppy)_2phi]Cl \cdot H_2O \cdot CH_2Cl_2$ with 50% probability ellipsoids. Hydrogen atoms are shown at arbitrary scale.

metalated complex was the relative positioning of nitrogen and carbon ligating atoms. The crystal structure of $[Rh(ppy)_2phi]$-Cl shows a distorted octahedron in which both of the 2-phenylpyridyl nitrogens are in axial positions, trans to one another. The 2-phenylpyridyl N−Rh−C bond angles are 80.66(9)° and 80.79(9)°. The N−Rh−N bond angle for the phi ligand is more acute at 73.92(8)° than the N−Rh−N bond angle between the two 2-phenylpyridyl nitrogens, which is 171.94(8)°. The bite angles of phi and ppy should be similar but the C−C bond between the two rings of ppy lends this ligand more flexibilty than is found in the more rigid phi. The bond angles between the 2-phenylpyridyl coordinating carbons and the phi ligand nitrogens are 102.72(9)°, 175.86(9)°, 95.25(9)°, and 169.05(9)°. As would be expected, the Rh−C σ-bond lengths of 1.996(3) and 2.003(2) Å are significantly shorter than the Rh−N dative bond lengths of 2.033(2) and 2.043(2) Å. The phi ligand is nearly planar with the torsion angles between C6−C7−C8−C9 and C2−C1−C14−C13 at −6.1(4) and −8.1(3)°, respectively. The 2-phenylpyridyl ligands are also nearly planar; the torsion angles within the ligands are all ≤4.0(4)°.

The phi ligands appear to be partially stacked in the crystal structure of $[Rh(ppy)_2phi]Cl$ (Supplementary Information). Other examples of structurally characterized octahedral metal complexes with phi ligands have been reported and show similar stacking of the diimine ligand.[21−23] One example, $[Rh(en)_2phi]$-$Br_3 \cdot 3H_2O$, is similar with nearly planar phi ligands that are partially stacked in the unit cell.[21] In this complex, the Rh−(phi)N bonds are 1.99(1) and 2.00(1) Å, the average of which is 0.053 Å shorter than the average Rh−(en)N bond length. The average Rh−(phi)N bond length of $[Rh(en)_2phi]Br_3$ is 0.136 Å shorter than the average Rh−(phi)N bond length of $[Rh(ppy)_2phi]Cl$, most likely because of the increased electron density on the rhodium in the cyclometalated complex.

The inverse trend is observed for $[Rh(ppy)_2phi]Cl$, for which the average Rh−(phi)N bond length is 0.10 Å longer than the corresponding average Rh−(ppy)N bond length. The (phi)N−Rh−(phi)N bond angle of 77.1(6)° for $[Rh(en)_2phi]Br_3$, like the difference between the Rh−N bond lengths, is between those found for $[Rh(bpy)_2chrysi]Cl_3$[24] and $[Rh(ppy)_2phi]Cl$. The X-ray crystal structures of $[Rh(NH_3)_4phi]^{3+}$, $[Rh([12]aneN_4)phi]^{3+}$, and $[Rh([12]aneS_4)phi]^{3+}$ have also been reported.[22] Partial π-stacking of the phi ligands is observed in these structures, where less overlap occurs in the complexes with bulkier ancillary ligands.

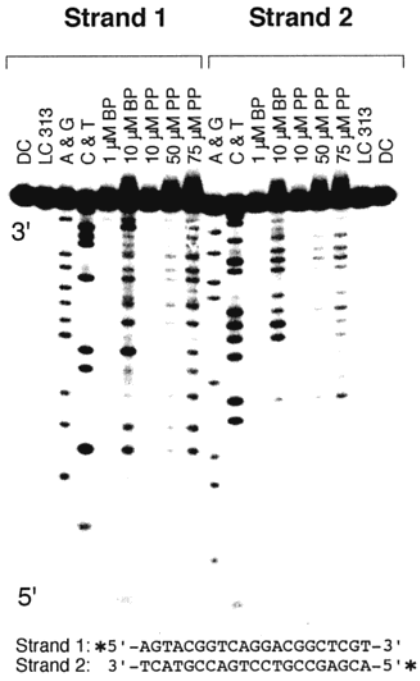

Figure 4. Phosphoimagery of a 20% polyacrylamide gel after DNA photocleavage by $[Rh(bpy)_2phi]Cl_3$ (BP) (1 and 10 μM) and $[Rh(ppy)_2phi]Cl$ (PP) (10, 50, and 75 μM) on a [5′-^{32}P]-labeled (indicated by *) B-form 21-mer (10 μM) duplex. All samples were prepared in 10 mM Tris pH 8.0, 2 mM NaOAc, 1.8 mM NaCl. All irradiations were at 313 nm for 15 min. Lanes labeled A&G and C&T refer to Maxam−Gilbert sequencing. DC refers to the dark control DNA sample without irradiation, and LC refers to the light control sample irradiated in the absence of metal complex.

The crystal structure of $[Rh(ppy)_2phi]Cl$ shows the complex to be structurally analogous to that of $[Rh(bpy)_2chrysi]Cl_3$,[21] as both are distorted octahedrons with all three bidentate ligands nearly planar. Another structure similar in shape is that of $[Ru(bpy)_2phi]^{2+}$, the first structurally characterized metal complex with a phi ligand. This complex is also a distorted octahedral complex with a nearly planar phi ligand and an average Ru−(phi)N bond length of 2.006 Å.[23] As expected, the substitution with cyclometalating 2-phenylpyridyl ligands for bipyridyl ligands does not significantly alter the shape of the complex.

Given the similarity of the overall dimensions of the ppy complexes in comparison to those of bpy complexes, one would expect the DNA binding characteristics to be similar for the two families of complexes. Indeed, such structural similarity may be evident in comparing the DNA binding and photocleavage properties of $[Rh(bpy)_2chrysi]Cl_3$ and $[Rh(ppy)_2chrysi]Cl$ in the presence of mismatched and Watson−Crick DNA (vide infra).

DNA Photocleavage by the Cyclometalated Complexes. DNA photocleavage by the phi complexes, $[Rh(ppy)_2phi]^+$and $[Rh(bpy)_2phi]^{3+}$, was first compared on a 21-mer DNA duplex with photoactivation at 313 nm. All samples were 10 μM in duplex, and samples containing Rh varied from 1 to 75 μM in metal complex. The photocleavage results were observed by phosphorimagery of the denaturing polyacrylamide gels (Figure 4).

(21) Schaefer, W. P.; Krotz, A. H.; Kuo, L. Y.; Shields, T. P.; Barton, J. K. *Acta Crystallogr.* **1992**, *C48*, 2071−2073.
(22) Krotz, A. H.; Kuo, L. Y.; Barton, J. K. *Inorg. Chem.* **1993**, *32*, 5963−5974.
(23) Pyle, A. M.; Chiang, M. Y.; Barton, J. K. *Inorg. Chem.* **1990**, *29*, 4487−4495.

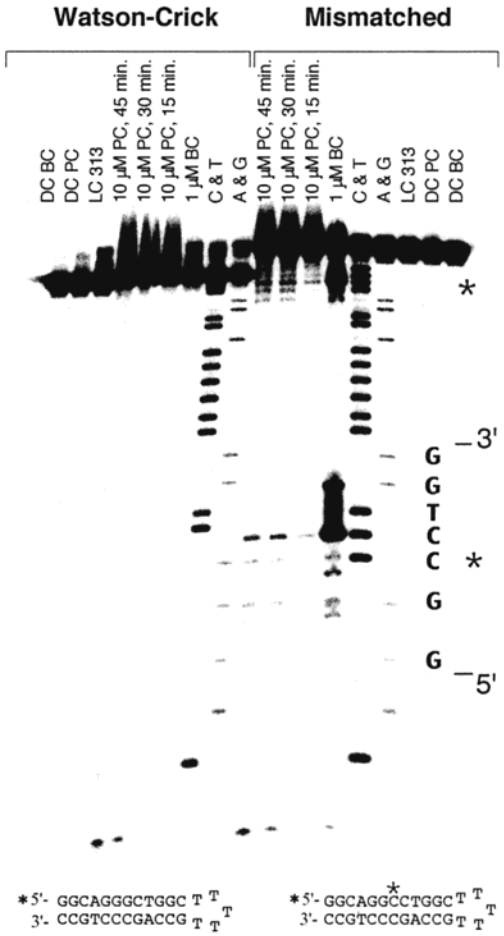

Figure 5. Phosphoimagery of a 20% polyacrylamide gel after DNA photocleavage by 1 μM [Rh(bpy)$_2$chrysi]Cl$_3$ (BC) and 10 μM [Rh(ppy)$_2$chrysi]Cl (PC) on [5′-^{32}P]-labeled (indicated by $*$) CC mismatch-containing (right) and Watson−Crick (left) 29-mer hairpins (1 μM). All samples were prepared in 10 mM Tris pH 8.0, 50 mM NaCl. All irradiations were at 313 nm (5 min for BC samples and 15, 30, or 45 min for PC samples). Lanes labeled A&G and C&T refer to Maxam−Gilbert sequencing. DC refers to the dark control DNA sample without irradiation, and LC refers to the light control sample irradiated in the absence of metal complex. The site of the mismatch is indicated by ★. The hairpin sequence is evident below. Note that the level of end-stacking, revealed as photocleavage visible at the 5′ end of the gel, increases with irradiation time.

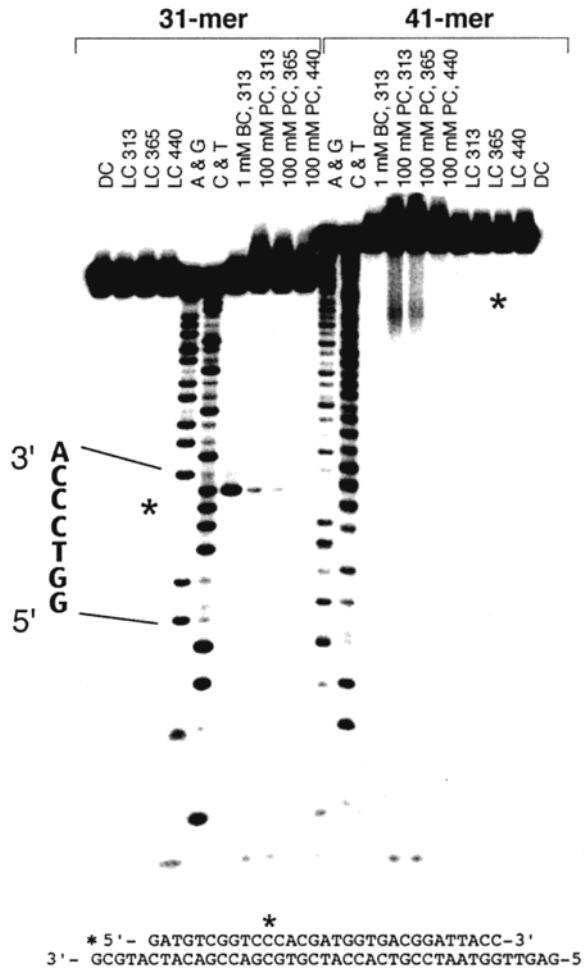

Figure 6. Phosphoimagery of a 20% polyacrylamide gel after DNA photocleavage by 1 μM [Rh(bpy)$_2$chrysi]Cl$_3$ (BC) and 100 μM [Rh(ppy)$_2$chrysi]Cl (PC) on a [5′-^{32}P]-labeled (indicated by $*$) CC mismatch-containing 31-mer/41-mer duplex (10 μM). Photocleavage is shown with (left) labeling of the 31-mer strand and (right) labeling of the 41-mer strand. All samples were prepared in 10 mM Tris pH 8.0, 2 mM NaOAc, 1.8 mM NaCl. Irradiations were at 313 nm for 5 min (bpy) or 15 min (ppy), 365 nm for 30 min, or 440 nm for 45 min. Lanes labeled A&G and C&T refer to Maxam−Gilbert sequencing. DC refers to the dark control DNA sample without irradiation, and LC refers to the light control sample irradiated in the absence of metal complex. The site of the mismatch is indicated by ★. Although the concentration of [Rh(ppy)$_2$chrysi]Cl is 10 times that in Figure 5, the decreased levels of photocleavage observed at the 5′ end of this gel indicate a decreased level of end-stacking.

[Rh(ppy)$_2$phi]$^+$, like [Rh(bpy)$_2$phi]$^{3+}$, promotes direct DNA strand scission upon high-energy irradiation. Furthermore, both complexes promote relatively nonspecific cleavage of the DNA. Some small variations in the pattern of cleavage between the two complexes at the higher metal concentrations are apparent. Particularly striking is the relative efficiency of cleavage by these complexes. Substantial cleavage with [Rh(ppy)$_2$phi]$^+$ was observed only at the highest concentration (75 μM) of metal complex, significantly higher than the 10 μM concentration sufficient for photocleavage by [Rh(bpy)$_2$phi]$^{3+}$.

DNA photocleavage by the chrysi analogues [Rh(ppy)$_2$chrysi]$^+$ or [Rh(bpy)$_2$chrysi]$^{3+}$ on 29-mer DNA hairpins (1 μM) either containing (MM) or lacking (WC) an internal CC mismatch was also compared. As is evident in Figure 5, the cyclometalated chrysi complex, [Rh(ppy)$_2$chrysi]$^+$ (10 μM), and to a much greater extent [Rh(bpy)$_2$chrysi]$^{3+}$ (1 μM), were capable of targeting the mismatch-containing DNA near the mismatched site, at the base(s) 3′ to the mismatch, when irradiated at 313 nm; no detectable photocleavage was found upon irradiation of the complexes in the presence of the DNA hairpin without the mismatch. Notably, however, even with the concentration of [Rh(ppy)$_2$chrysi]$^+$ 10-fold that of [Rh(bpy)$_2$chrysi]$^{3+}$ and the irradiation time increased 3-fold, the level of damage induced by [Rh(ppy)$_2$chrysi]$^+$ was small compared to that by [Rh(bpy)$_2$chrysi]$^{3+}$. Indeed, comparable damage was observed only when the concentration of the cyclometalated complex was increased to 50-fold that of [Rh(bpy)$_2$chrysi]$^{3+}$ and the irradiation time increased 3-fold (data not shown). It should be noted that the damage evident at the bottom of the gel is most likely due to end-stacking of the chrysi complexes on the hairpin. This damage increases with irradiation time and/or concentration and is found on both the mismatched and Watson−Crick hairpins.

Shown in Figure 6 is a gel comparing the damage induced on a 31/41-mer duplex (10 μM) by either 1 μM [Rh(bpy)$_2$chrysi]$^{3+}$ upon irradiation at 313 nm or 100 μM [Rh(ppy)$_2$chrysi]$^+$upon irradiation at 313, 365, or 440 nm. Here too, the photocleavage observed for the cyclometalated complex

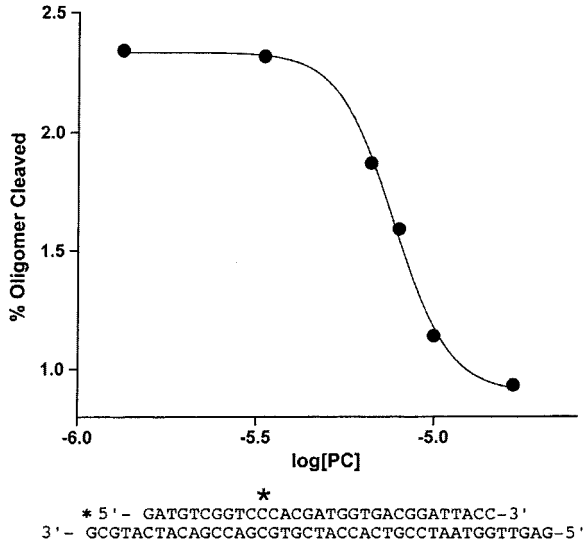

Figure 7. Plot of competitive binding of $[Rh(bpy)_2chrysi]Cl_3$ vs $[Rh(ppy)_2chrysi]Cl$. Shown is the % photocleavage by $[Rh(bpy)_2chrysi]^{3+}$ in the presence of increasing concentrations of $[Rh(ppy)_2chrysi]^+$. Irradiations were at 440 nm for 15 min each. Samples were mismatch-containing DNA (1 μM) and $[Rh(bpy)_2chrysi]Cl_3$ (1 μM) with increasing concentrations of $[Rh(ppy)_2chrysi]Cl$ (1−25 μM). All samples were in 10 mM Tris, 50 mM NaCl, pH 8.0.

is much less than that found with $[Rh(bpy)_2chrysi]^{3+}$, even though the concentration of the bpy analogue is 100-fold lower. Here, little damage at the ends is evident, especially given the 100 μM concentration of the cyclometalated complex; this is consistent with the decreased ability of the chrysi complexes to end-stack when the ends of the duplex are uneven. Furthermore, no significant photocleavage is evident in the single-stranded region.

To probe to what extent the lower efficiency of cleavage with the cyclometalated analogue is a function of a lower level of binding by the monocationic complex compared to the tricationic bpy analogue, competitive binding studies were carried out on the 31/41-mer duplex using the photocleavage assay. Here the amount of $[Rh(ppy)_2chrysi]^+$ necessary to outcompete cleavage by the $[Rh(bpy)_2chrysi]^{3+}$ complex was monitored. The mismatch-containing DNA duplex was treated with both $[Rh(bpy)_2chrysi]^{3+}$ at constant concentration and $[Rh(ppy)_2chrysi]^+$ in increasing concentrations up to 50 times the concentration of $[Rh(bpy)_2chrysi]^{3+}$ and then irradiated at 440 nm. This wavelength was chosen because the cyclometalated complex does not promote photocleavage at 440 nm whereas the photocleavage by $[Rh(bpy)_2chrysi]^{3+}$ is strongest at this wavelength. At 313 nm, however, photocleavage induced by the cyclometalated complex would have been indistinguishable from the photocleavage that was being monitored.

Figure 7 shows a plot of the ratio of the intensity of the photocleavage observed at the mismatch site over the intensity of the DNA parent band versus the log of the concentration of $[Rh(ppy)_2chrysi]^+$ added. The curve obtained appears to be characteristic of competitive binding. The midpoint concentration, indicative of the concentration of $[Rh(ppy)_2chrysi]^+$ where 50% of bound $[Rh(bpy)_2chrysi]^+$ has been displaced, corresponds to a concentration of 9×10^{-6} M, or a ratio of approximately 14:1 $[Rh(ppy)_2chrysi]^+$ to $[Rh(bpy)_2chrysi]^{3+}$.

An analogous competitive binding study was conducted in which $[Rh(ppy)_2phi]^+$ and $[Rh(bpy)_2phi]^{3+}$ photocleavage effects were compared on a B-form duplex. A roughly comparable result was obtained (data not shown). However, because the complexes promote photocleavage at many sites, the analysis in this case has a higher associated uncertainty.

Discussion

Synthesis of $[Rh(ppy)_2phi]Cl$ and $[Rh(ppy)_2chrysi]Cl$. Cyclometalated analogues of rhodium intercalators have now been prepared and structurally characterized. The cyclometalating ligand 2-phenylpyridine was chosen for this study because it is isostructural with bipyridine and coordinates using both the carbanion and nitrogen donor. Thus, although the overall shape of the complex resembles that of the bpy analogue, the overall charge of a bis(cyclometalated) analogue of a bis(bipyridine) complex is lowered by 2 units.

$[Rh(bpy)_2chrysi]^{3+}$ can be synthesized in high yield via condensation of chrysenequinone with $[Rh(bpy)_2(NH_3)_2]^{3+}$, which is generated from the ditriflate, $[Rh(bpy)_2(OTf)_2]^+$.[24] However, the synthesis of the cyclometalated analogues could not be carried out using a parallel scheme to that employed for the bpy complex;[25] treatment of $[Rh(ppy)_2Cl]_2$ with neat triflic acid to form the cyclometalated analogue of the ditriflate, $[Rh(ppy)_2(OTf)_2]^-$, resulted in decomposition, most likely because of protonation of the 2-phenylpyridyl ligands to regenerate 2-phenylpyridine. Consequently, $[Rh(ppy)_2phi]^+$ and $[Rh(ppy)_2chrysi]^+$ were prepared by an alternative route; the dichlorodimer $[Rh(ppy)_2Cl]_2$ was treated with either 9,10-diaminophenanthrene or 5,6-diaminochrysene to form their respective diimino complexes, $[Rh(ppy)_2phi]^+$ and $[Rh(ppy)_2chrysi]^+$.

Structural Characterization of $[Rh(ppy)_2phi]Cl$. Although cyclometalated complexes of Rh(III) and Ir(III) have been studied extensively, few such complexes with 2-phenylpyridyl ligands have been structurally characterized.[26] Some examples using 2-phenylpyridine or its derivatives as C∧N cyclometalating ligands include $[Rh(thpy)_2(bpy)]$ (thpy = 2-(thien-2-yl)-pyridine),[27] $[Rh(bpy)_2(ppy)][PF_6]_2$,[28] $[Rh(Br\text{-}ppy)_2Cl]_2$ (Br-ppy = (5′-bromo-2′-(2-pyridyl)phenyl),[29] $[Ir(ppy)_2(4mptr)][PF_6]$ (4mptr = 4-methyl-3-(pyridin-2-yl)-1,2,4-triazole),[30] and $[Ir(ppy)_2(cpbpy)][PF_6]$ (cpbpy = 4′-(4-carboxyphenyl)-6′-phenyl-2,2′-bipyridine).[31]

Of these examples, the most relevant to $[Rh(ppy)_2phi]Cl$ is $[Rh(thpy)_2(bpy)]$ because they are both monomeric rhodium complexes chelated by two cyclometalating ligands. In this structure, as well as in the structures of $[Rh(bpy)_2(ppy)][PF_6]_2$,

(24) Murner, H.; Jackson, B. A.; Barton, J. K. *Inorg. Chem.* **1998**, *37*, 3007−3012.
(25) $_2(NH_3)_2]^+$ has been synthesized and structurally characterized (Junicke, H.; Barton, J. K. Manuscript in preparation.). However, the attempted condensation of $[Rh(ppy)_2(NH_3)_2]^+$ and chrysenequinone, analogous to that used to synthesize the diimine complex $[Rh(bpy)_2chrysi]^{3+}$, has not yet successfully yielded the diimine of the cyclometalated complex, $[Rh(ppy)_2chrysi]^+$. Thus, an alternative synthetic method was employed.
(26) Other structurally characterized examples of complexes with phenylpyridyl or benzo[*h*]quinolyl cyclometalating ligands include square planar platinum and mercury complexes: (a) Chassot, L.; Muller, E.; von Zelewsky, A. *Inorg. Chem.* **1984**, *23*, 4249. (b) Deuschel-Cornioley, C.; Stoeckli-Evans, H.; von Zelewsky, A. *J. Chem. Soc., Chem. Commun.* **1990**, 121. (c) Black, D. St. C.; Deacon, G. B.; Edwards, G. L.; Gatehouse, B. M. *Aust. J. Chem.* **1993**, *46*, 1323.
(27) Maeder, U.; von Zelewsky, A.; Stoeckli-Evans, H. *Helv. Chim. Acta* **1992**, *75*, 1320−1332.
(28) Constable, E. C.; Leese, T. A.; Tocher, D. A. *Polyhedron* **1990**, *9*, 1613−1616.
(29) Fronczek, F. R.; Gutierrez, M. A.; Selbin, J. *Cryst. Struct. Commun.* **1982**, *11*, 1119.
(30) Van Diemen, J. H.; Haasnoot, J. G.; Hage, R.; Muller, E.; Reedijk, J. *Inorg. Chim. Acta* **1991**, *181*, 245.
(31) Neve, F.; Crispini, A.; Campagna, S.; Serroni, S. *Inorg. Chem.* **1999**, *38*, 2250−2258.

$[Ir(ppy)_2(4mptr)][PF_6]$, $[Ir(ppy)_2(cpbpy)][PF_6]$, and the dimeric $[Rh(ppz)_2Cl]_2$,[1a] it was observed that the 2-phenylpyridyl, or phenylpyrazolyl, nitrogens are trans to each other and the coordinating carbons are cis to each other. However, the structure of $Ru(bzq)_2(CO)_2$ (bzq = benzo[*h*]quinolin-10-yl)[32] shows the benzo[*h*]quinolyl nitrogens to be coordinated cis to each other.

In the case of $[Rh(ppy)_2phi]Cl$, the symmetry indicated by the singlet ^1H NMR resonance corresponding to the imino protons of the phi ligand suggested that both 2-phenylpyridyl ligands have the same orientation, with either cis or trans nitrogens. Therefore, further structural characterization was found to be necessary.

As in the structure of $[Rh(thpy)_2(bpy)]$, the structural characterization of $[Rh(ppy)_2phi]Cl$ revealed the nitrogens of the cyclometalating ligands to be trans nitrogens with Rh−N bond lengths of 2.033(2) and 2.0439(19) Å. As would be expected, the Rh−C bonds are shorter, and the differences between the Rh−N and Rh−C bond lengths are 0.037 and 0.0409 Å. These values are smaller but comparable to those of 0.071 and 0.072 Å for $[Rh(thpy)_2(bpy)]$; here, increased back-bonding might account for the additionally decreased Rh−C bond lengths. For $[Ir(ppy)_2(4mptr)][PF_6]$, the average Ir−C and Ir−N bond lengths for the 2-phenylpyridyl ligands are 2.01 and 2.05 Å, respectively. The average difference between Rh−N and Rh−C bond lengths of 0.04 Å is in agreement with that found for $[Rh(ppy)_2phi]Cl$. The average difference between Rh−N and Rh−C bond lengths for $[Rh(ppz)_2Cl]_2$, in which the cyclometalating ligands are 2-phenylpyrazolyl units, is also very similar to that of $[Rh(ppy)_2phi]Cl$ at 0.036 Å. The difference between N and C bond lengths is likely due to the Rh−C σ-bonds increasing electron density on the metal center.

This trans disposition of N-coordinating ligands will be valuable in building novel metal complexes for site-specific recognition. The trans-directing effects of the cyclometalated ligands greatly simplify the isolation of a specific isomer of an intercalator containing nonsymmetric bidentate ligands. Owing to the problem of separating multiple isomers, we have focused thus far primarily on the construction of metallointercalators using symmetric ligands. The use of cyclometalated (C∧N) ligands obviates that requirement. Indeed the positioning of the cyclometalated ligands around the metal center should considerably facilitate the isolation of intercalators containing asymmetric ligands that might be favorable for sequence-specific recognition.

DNA Binding and Photocleavage. In addition, the cyclometalated analogue of $[Rh(bpy)_2chrysi]^{3+}$ was synthesized to lower the charge of the complex while retaining its overall shape and reaction selectivity for base pair mismatches. As has been evidenced by the crystal structure of $[Rh(ppy)_2phi]^+$ in comparison to that of $[Rh(bpy)_2chrysi]^{3+}$, the bis(bipyridyl) complexes and their cyclometalated analogues, although they differ in charge, are very similar in overall shape. Because intercalation at the mismatch is based upon shape selectivity, it was expected that the cyclometalated complex $[Rh(ppy)_2chrysi]^+$ would target mismatches similarly to $[Rh(bpy)_2chrysi]^{3+}$. Indeed, specific targeting of a mismatch site by $[Rh(ppy)_2chrysi]^+$ is achieved. Furthermore, competitive binding studies were conducted and showed that the binding to DNA by the cyclometalated complex was decreased by only a factor of 14; the thermodynamic binding constant of Δ-$[Rh(bpy)_2chrysi]^{3+}$ for the CC mismatch site in the 35-mer DNA hairpin is 8×10^5 M^{-1}.[13a] Thus, on comparison of affinities of the trivalent and monovalent cations, it is clear that intercalation here does not appear to be largely dominated by electrostatics.

The competitive binding studies also highlight the difference in photoefficiency between the bpy and ppy analogues. Approximately 50 times the concentration of the cyclometalated complex was required, in addition to a 3-fold greater irradiation time, to achieve a level of photocleavage comparable to that of $[Rh(bpy)_2chrysi]^{3+}$. Similar values were observed in comparing damage induced by $[Rh(bpy)_2phi]^{3+}$ to that induced by $[Rh(ppy)_2phi]^+$. Thus photoefficiencies of the cyclometalated complexes must be lower than those of their noncyclometalated counterparts. Because the metal−carbon σ-bonds of the cyclometalated complexes result in greater electron density at the metal center, such a trend would be expected if photocleavage occurs via the abstraction of a hydrogen atom from a backbone sugar by the excited intercalating ligand. The LMCT transitions of the cyclometalated complexes are higher in energy than those of $[Rh(bpy)_2phi]^{3+}$ and $[Rh(bpy)_2chrysi]^{3+}$.

Conclusions

The synthesis of cyclometalated Rh(III) complexes provides a starting point for the study of a new family of metallointercalators. The structural characterization of $[Rh(ppy)_2phi]^+$ by X-ray diffraction shows that the 2-phenylpyridyl nitrogens are trans to each other and all three ligands are nearly planar in a distorted octahedron, rendering the cyclometalated complex structurally similar to the bis(bipyridyl) analogue, $[Rh(bpy)_2phi]^{3+}$. Because of such trans-directing effects, single isomers of Rh(III) intercalators with nonsymmetric (C∧N) cyclometalating ancillary ligands can be isolated readily. These studies furthermore show that cyclometalated complexes of Rh(III) can intercalate in DNA and induce strand scission of the DNA backbone in the presence of UV light. Analogously to their bpy counterparts, the complex $[Rh(ppy)_2chrysi]^+$ can effectively target base pair mismatches and $[Rh(ppy)_2phi]^+$ photocleaves canonical B-DNA as well as mismatched DNA. It has also been found that the cyclometalated complex $[Rh(ppy)_2chrysi]^+$ has an approximately 14-fold decreased affinity for base pair mismatches than does $[Rh(bpy)_2chrysi]^{3+}$, most likely because of the lower charge on the cyclometalated complexes. In addition, the decreased levels of damage observed compared to those of the +3 charged analogue indicate a lower photoefficiency for the cyclometalated complex. These cyclometalated intercalators represent the foundation for a new family of complexes targeted to DNA where highly sequence-specific design should be feasible for chemotherapeutic applications.

Acknowledgment. We gratefully acknowledge the National Institutes of Health (GM33309) for financial support of this work and for a postdoctoral fellowship to J.L.K. We are also grateful to Lawrence M. Henling at the Caltech X-ray Crystallography Laboratory for his technical expertise, and we thank D. T. Odom, H. Junicke, and M. Pascaly for helpful discussions.

Supporting Information Available: Final atomic coordinates (Table S1), bond lengths and angles (Table S2), anisotropic displacement parameters (Table S3), hydrogen coordinates and isotropic displacement parameters (Table S4), torsion angles (Table S5), hydrogen bond data (Table S6), and a view of crystal packing (Figure S1). This material is available free of charge via the Internet at http://pubs.acs.org.

IC000549Z

(32) Patrick, J. M.; White, A. H.; Bruce, M. I.; Beatson, M. J.; Black, D. St. C.; Deacon, G. B.; Thomas, N. C. *J. Chem. Soc., Dalton Trans.* **1983**, 2121.